Study of Breakup Mechanisms in Cavity Flow

John Kang and Theodore G. Smith
Chemical Engineering Dept., University of Maryland, College Park, MD 20742

David I. Bigio
Mechanical Engineering Dept., University of Maryland, College Park, MD 20742

Drop breakup mechanisms inside a cavity flow are presented for two immiscible fluids. Due to the nonuniform flow condition of the cavity, the breakup mechanism varied along the streamlines. The streamlines were characterized by stream zones A and B, where zone A possessed a methodical transient breakup governed by Tomotika's breakup via capillary instabilities, and the breakup mechanism of stream zone B consisted of tip streaming breakup, an inefficient breakup mechanism. The flow behavior near flight region had a significant role in the drop breakup mechanisms. The study of the evolution of drop dispersion showed that the matrix viscosity is critical in controlling the transient breakup process and that the shear rate increase had little or no effect on the drop breakup.

Introduction

Most useful plastic products are mixtures of pure polymers or copolymers with a variety of additives. Recently, considerable attention has been placed on the processing of polymer blends which give products of unique properties. The detailed morphological structure of the blends depends on component rheologies, polymer properties, and the nature of mixing mechanisms, which are related closely to the mixing geometry and operating conditions. The polymer blending is governed primarily by dispersive mixing which involves rupture and distribution of a minor phase into a matrix phase. Well-known examples of dispersive mixing processes include the mixing operation of carbon black into rubber, where carbon black, the minor component, has direct influences on the mechanical properties. Also, polybutylene-terephthalate (PBT) can improve its property by blending with acrylonitrile-butadiene-styrene (ABS), ethylene-propylene-diene (EPDM), and other rubber for toughness (Ulrich, 1993). Also, a third minor component can be added to the interface of blends to attain uniform and stable morphologies, as shown in Figure 1. Therefore, if dynamics of immiscible mixing can be understood in greater detail, the application of the third minor component can be improved and the blend morphology can be controlled more effectively.

Correspondence concerning this article should be addressed to D. I. Bigio.
Current address of J. Kang: Union Carbide Corp., P.O. Box 670, Bound Brook, NJ 08805.

Theory

The study of drop deformation and breakup was investigated originally by G. I. Taylor (1934) to understand the physics behind the formation of emulsions in definable flow fields. Since then, many theoretical and experimental studies have followed on the drop deformation and breakup in the pure extensional and simple shear flows to predict the mixing of immiscible fluids in real systems with complex flow fields. The notable experiments by Rumscheidt and Mason (1961), by Karam and Bellinger (1968), by Grace (1982), and by Tjahjadi and Ottino (1991) and reported that the behavior of drops was found to depend on the combination of flow field characteristics and viscosity ratio.

Taylor developed the expression which predicted the deformability of a drop in steady shearing flow field as

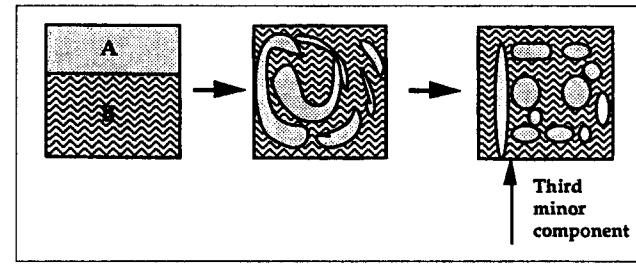

Figure 1. Immiscible mixing process.

$$\frac{L-B}{L+B}=\frac{2G\eta_m R}{\sigma}\left(\frac{19\eta_r+16}{16\eta_r+16}\right) \tag{1}$$

where L and B are the measured value of the half length and half breadth of the drop, G is the shear rate, R is the drop radius, σ is the interfacial tension, η_m is the matrix viscosity, and η_r is the viscosity ratio of the dispersed to matrix phase. This relationship was shown to be valid only in the initial deformational state, and deviated gradually as the drop elongated further. Attempts have been made to improve the deformability expression as Elemans (1993) showed the deformability as a function of the total strain

$$\frac{L-B}{L+B}=\left[\frac{(1+\gamma^2)^{3/4}-1}{(1+\gamma^2)^{3/4}+1}\right] \tag{2}$$

Taylor's theoretical estimate, based on the hydrodynamic equations, says that there is a maximum drop size the surface tension of drop expects to hold together against a given viscous drag force. This relationship is represented by the capillary number Ca where

$$Ca=\frac{G\eta_m R}{\sigma}>Ca_{\text{crit}} \tag{3}$$

The critical capillary number Ca_{crit} which can be obtained empirically by determining the minimum shear rate that causes breakup for a given drop size is represented as a function of the viscosity ratio and type of flow field. Equation 3 states that for given drop size and viscosity ratio, if the ratio of viscous force to interfacial tension is greater than Ca_{crit} then breakup will occur. Figure 2 gives Ca_{crit} curves plotted in terms of viscosity ratio for an extensional flow and a simple shear flow. The figure depicts the strong dependence of

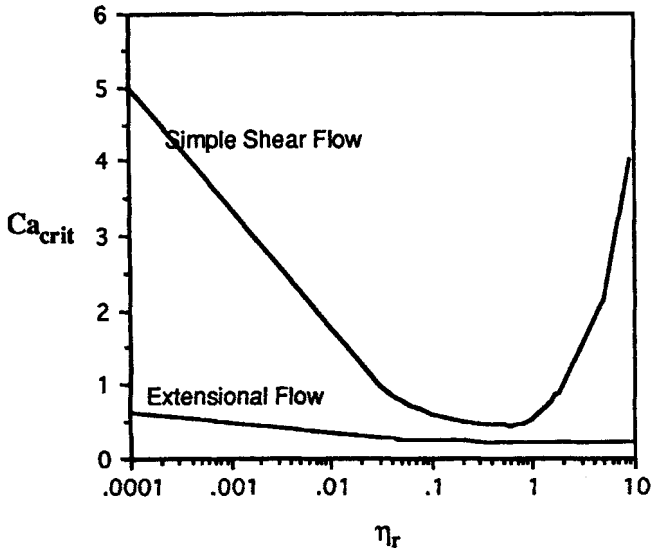

Figure 2. Critical capillary number vs. viscosity ratio for simple shear and extensional flow.
DeBruijn (1989).

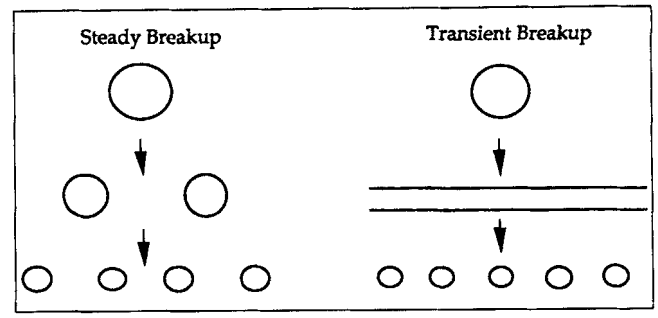

Figure 3. Steady and transient breakup mechanisms.

Ca_{crit} (drop breakup) on the flow type. Although both flow types reach the minimum, Ca_{crit} at the range of $\eta_r \sim 0.1$ to 1.0; as η_r deviates from this range, the shear flow becomes more strongly dependent on η_r than the extensional flow. For a real system, Eq. 1 is limited to the application of average G and R values since the local shear rate or local drop size cannot be determined easily and traced along the flow field; therefore, it is possible to misinterpret a breakup process based on the average values of G and R.

Whereas Taylor's theoretical construction has been applied constantly to flowing systems, other breakup mechanisms have been observed experimentally during flow cessation (see Figure 3). Taylor (1934) and Rumscheidt and Mason (1961) observed that a drop, which did not breakup for a modest extension, broke up into equally sized drops following the cessation of flow.

Also under unsteady shear conditions, more effective breakups have been reported under unsteady shear conditions than under steady conditions. Torza et al. (1970) found that the drop breakup mechanism seems to depend largely upon the rate of increase of shear rate. In the case of a Newtonian dispersed phase in a viscoelastic continuous phase, Flumerfelt (1972) found that both the minimum drop size and the critical shear rate decreased significantly under an unsteady shear condition as compared to a steady condition. Also, Shi and Utracki (1992) have postulated a transient breakup in a twin screw extruder as transition from a high shear to low shear zone occurs. These observations attest that the drop breakup of immiscible fluid systems are more effectively achieved under a transient shear flow condition, and a theory other than Taylor's steady breakup theory is necessary for explaining the breakup under transient flow conditions.

The breakup under a transient shear condition can be explained extensively by Tomotika (1936), who indicated that a long cylindrical thread formed upon shearing develops sinusoidally capillary instabilities when it is placed under a quiescent flow (unsteady condition) and is allowed to relax as shown in Figure 4. According to the theory, if $\lambda_m < 2\pi a$ then the capillary disturbance is dampened, while if $\lambda_m \geq 2\pi a$, the instabilities continue to grow and lead to disintegration of the thread into equally sized small drops. The growth of capillary instabilities is governed by the growth factor q which is defined as

$$q=\frac{\sigma}{2\eta_m a}(1-x^2)\phi(x,\eta_r) \tag{4}$$

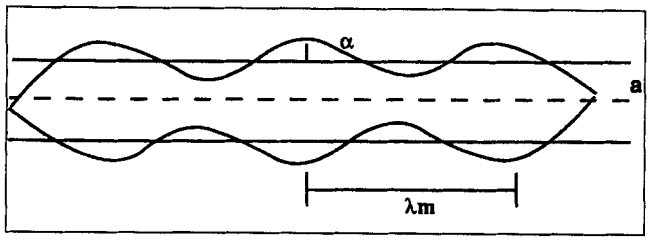

Figure 4. Thread disturbed by capillary instability.

a is the mean thread radius, α is the disturbance amplitude, and λ_m is the dominating wavelength.

where $x = 2\pi a/\lambda$ is called the wave number and $\phi(x, \eta_r)$ is the complex function obtained from the solution of the creeping motion equations for an incompressible fluid

$$\eta \nabla^2 u + \nabla p = 0 \tag{5a}$$

$$\nabla \cdot u = 0 \tag{5b}$$

Tomotika assumed that once the capillary force governs the breakup, the wave number associated with the maximum instability $x_m = 2\pi a/\lambda_m$ dominates the instability process. As the maximum instability grows, the amplitude of disturbance grows exponentially with time as

$$\alpha = \alpha_0 e^{qt} \tag{6}$$

where Kuhn (Janssen and Meijer, 1993) approximated the cause of the initial disturbance α_0 as thermal fluctuations

$$\alpha_0 = \left(\frac{21kT}{8\pi^{3/2}\sigma} \right)^{1/2} \tag{7}$$

where k is Boltzmann's constant and T is absolute temperature. The initial disturbance corresponds to the condition when the extended thread just becomes unstable and begins to develop the capillary instabilities. The radius of drop R produced by the breakup can be obtained using the conservation of volume as:

$$\left(\frac{R}{a_0} \right) = \left(\frac{3\pi}{2} \right)^{1/3} \frac{e^{-\epsilon t/2}}{(x_m)^{1/3}} \tag{8}$$

where a_0 is the initial thread radius, x_m is the dominant wave number, and ϵ is the extensional rate. In the quiescent flow by rearranging Eq. 1, the breakup time related to the capillary instability can be expressed as

$$t_b = \frac{1}{q} \ln \frac{a}{\alpha_0} \tag{9}$$

Additionally, the studies (Tomotika, 1936; Mikami et al., 1975; Janssen and Meijer, 1993) of breakup of a thread extending at a constant rate have shown that a presence of flow suppresses the growth of capillary instabilities until the thread had thinned out substantially, at which time much smaller droplets can be produced.

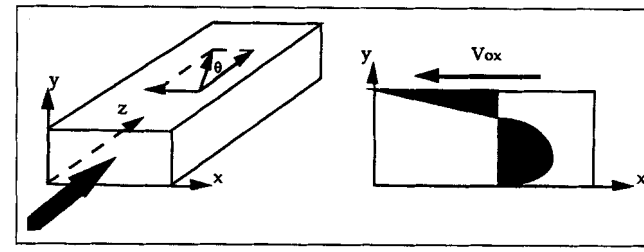

Figure 5. Flow through a rectangular duct with a moving top plate at an angle θ simulates the flow field of single-screw extruder.

The transverse flow is the flow component in xy-plane.

Taylor's theory has been used both experimentally and analytically as a basis for understanding the immiscible polymer mixing process and has been extended to applications where the flow field is not steady, while Tomotika's theory appears to adequately model the breakup phenomenon during the cessation of flow. We propose to extend the application of Tomotika's approach as a basis for modeling morphological development in a constantly changing flow field, as would be formed in a simple rectangular cavity flow.

Breakup Analysis in 2-D Cavity Flow

In this study, an attempt is made to delineate drop breakup mechanisms inside a 2-D cavity to simulate the flow of the single screw extruder as shown in Figure 5. The single-screw extruder is considered as a poor mixer mainly due to lack of high shear regions which is essential for achieving $Ca > Ca_{crit}$ to induce breakup. Although Taylor et al. have conducted experimental studies in simple flow fields to interpret real systems, these studies are not fitted for describing the mixing of numerous drops in a complex flow field such as the flow field of the single-screw extruder.

Apparently, the Tomotika theory, which explains the breakup mechanism under an unsteady flow condition, is more suited for explaining the transient nature of the single-screw extruder, where the transient flow induces drop breakups even though drops may not experience the critical condition of $Ca \geq Ca_{crit}$.

In the 2-D cavity, since the flow field consists of streamlines with varying flow conditions, the drop morphology across the cavity channel is not expected to be uniform. Hence, it is a goal of this study to discern how different stress histories along the streamlines influence breakup mechanism and to explain the breakup mechanisms based on the nature of flow characteristics in different regions of the cavity. Figure 6

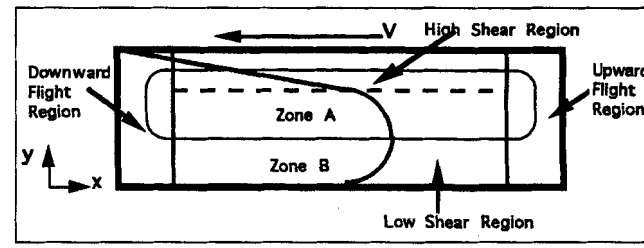

Figure 6. Four distinct flow regions and stream zones A and B in the cavity channel.

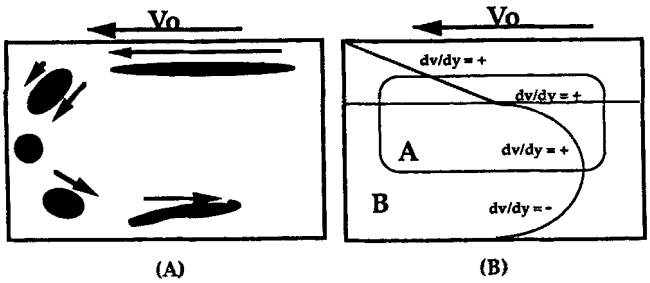

Figure 7. (A) Inversion of shear direction caused the drop to collapse in the flight region (→, relative stress tensor); (B) in zone A, the shear direction remains constant relative to flow as the drop moves from the upper to lower region, while the opposite is true in zone B.

shows that the cavity is divided into four regions, which include high shear, low shear, and downward and upward flight regions. Also, with nonuniform condition across the cavity channel, we propose to divide the streamlines into two zones, zone A and B, where the zones are separated by the streamline which passes through the zero shear line at $y^* = 1/3$ ($dVx/dy = 0$). This streamline is chosen to separate the two zones since the flow characteristics of the streamlines diverge as you move away from this streamline and, thus, affect the breakup mechanism. Ideally, along this streamline, an elongated drop flowing through the low shear region develops the capillary instability induced by the zero shear stress condition at $y^* = 1/3$, and then breakups occur as discussed by Tomotika. Based on this Tomotika breakup mechanism, the breakup phenomena in stream zone A and B will be discussed in detail.

Stream zone A

The breakup mechanism in stream zone A portrays the typical Tomotika breakup described earlier, where a drop elongates in the high shear region, and then develops the capillary instability in the low shear region and leads to the Tomotika breakup where droplets of similar size are produced. This breakup mechanism is most efficient near the zero shear streamline, and the efficiency of the transient nature of flow decreases as the drop nears $y^* = 2/3$, where the transient nature of flow is extinct. It is also important to mention the influence of the flight regions have on the breakup mechanisms. In this study, it has been observed that the flow characteristics in the downward flight region appear to disrupt the breakup mechanism as the drop travels from the high shear to low shear region. Connor (1989) showed in his numerical study of mixing cavity flow that the flight regions promote de-stretching (de-mixing). In general, zone A possesses fluent breakup processes due to an effective transient flow condition and negligible effect by the downward flight region.

Figure 9 shows the magnitude of shear stress along the arbitrarily chosen streamlines in stream zone A and B obtained from the Kantorovich and Galerkin Method (Chella and Ottino, 1985) which gives the semianalytical solution to the rectangular cavity flow. In Figure 9, it is important to note that the magnitude of shear stress in zone A reduced gradually

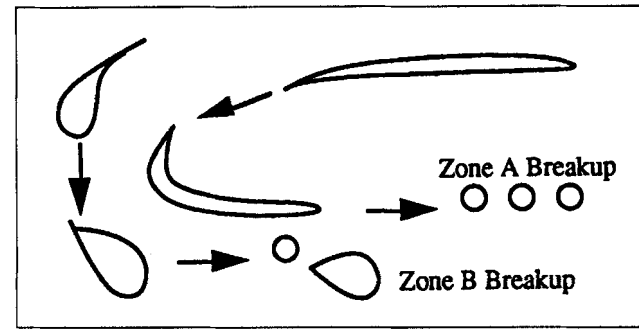

Figure 8. Breakup mechanisms in zone A and B.

from the high to low shear region, while reaching the minimum in the low shear region; however, in zone B, the shear stress reduces to the minimum in the flight region before the stress level gradually increases again in the low shear region.

Stream zone B

The effectiveness of the Tomotika breakup mechanism in stream zone B is reduced substantially due to differences in the flow characteristics compared to stream zone A. The shear stress history of zone B can be described as follows: a drop flowing in this stream zone sees a high shear stress in the high shear region followed by an abrupt shear stress decrease in the downward flight region, and then the drop experiences gradual increase in shear stress in the low shear region. In this zone, the Tomotika breakup mechanism is suppressed due to the downward flight region where the sudden decrease in shear stress disrupts the relaxation process resulting in either no breakup or an undesired breakup mechanism, such as tip streaming breakup where small drops are shed off from the tip of the main drop, as illustrated in Figure 8. Also, in zone B, the breakup condition worsens as you move further away from the zero streamline as the duration in the downward flight region increases and the shear stress in the low shear region also increases; hence, the transient nature of flow diminishes.

Moreover, a drop flowing through the downward flight region changes its direction of shearing and this phenomenon further hinders a smooth transition from the high shear to low shear region. Tjahjadi and Ottino (1991) showed that a change in sign of shearing causes the drops to form large

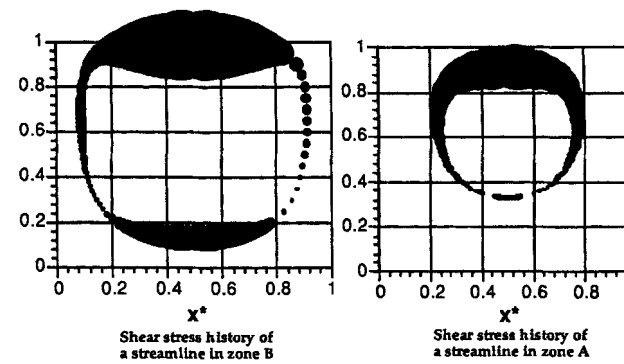

Figure 9. Shear stress history of streamlines in zone A and B.

The size of bubbles indicates the magnitude of stress.

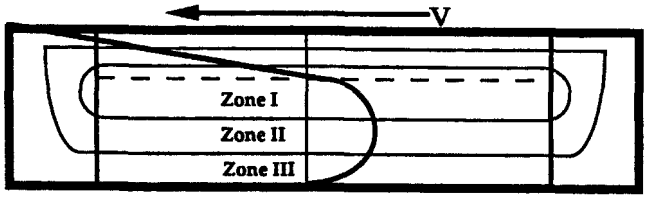

Figure 10. Stream zones I, II, and III.

drops, and hinders conventional capillary instability breakups. This effect is depicted in Figure 7, as the change in shearing direction seems to allow coalescence of the drops to occur more easily, and the drops to collapse to a spherical form in the downward flight.

Zone I, II and III

To take a different approach, the cavity may be divided into three stream zones as shown in Figure 10. In this approach, the focus is directed on zone II, where the shear stress is close to zero value in the low shear region since the zone is centered around the zero shear line of $y^* = 1/3$. Because Tomotika's theory requires a quiescent flow after the drop has been extended, the flow condition of zone II may best satisfy the flow criterion of Tomotika's breakup phenomenon. The breakup phenomenon in this zone can be observed and compared to the Tomotika's model. The breakup phenomena in zones I and III are insignificant since these zones make up the poor breakup regions in zones A and B.

Experimentation

The experimental 2-D cavity is made of Plexiglas for a clear viewing, and consists of $W = 12$ cm and $H = 2$ cm, where the aspect ratio is $W/H = 6$. Also, the depth of 2 cm is confirmed numerically and experimentally to be sufficient for the 2-D study. (Specifications of the experimental cavity are shown in Figure 12.) The expression for the fully-developed drag velocity profile of the top plate is given by Rowell and Finlayson (1922) as

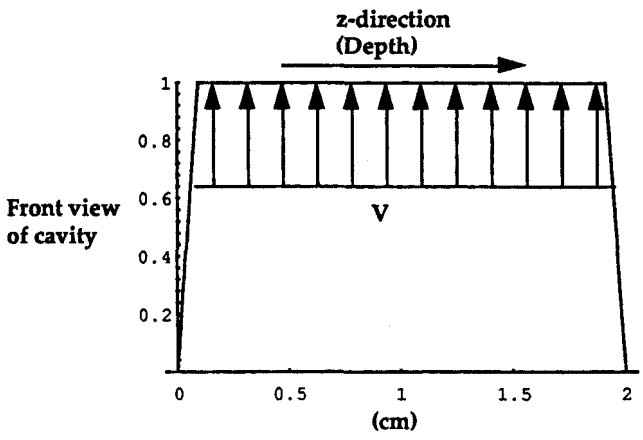

Figure 11. Fully developed velocity profile of the top plate.

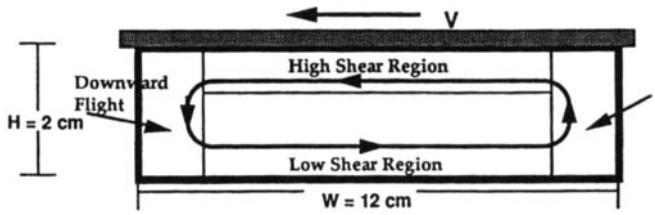

Figure 12. Specifications of the experimental cavity.

$$V_d(x_1, x_2) = \frac{4V_0}{\pi} \sum_{i=1,3,5\ldots}^{\infty} \frac{\sinh(i\pi x_2/W)}{i \sinh(i\pi H/W)} \sin(i\pi x_1/W) \tag{12}$$

Using Eq. 12, the velocity profile of the top plate is obtained as in Figure 11, which shows that there is no significant disturbance on the two dimensionality of the flow.

The experimental fluids consist of Glycerin as the dispersed phase and polydimethylsiloxane (PDMS) as the matrix phase. Table 1 gives the detailed properties of the fluid system.

The interfacial tension between the silicone oil and Glycerin is found to be 25 dynes/cm (Rumscheidt and Mason, 1961; Dann, 1970), which is determined by the pendant drop method and Taylor's deformation theory. Experiments are operated at the room temperature of 25°C and both Glycerin and the silicone oil were assumed a Newtonian fluids. While Glycerin is inherently a Newtonian fluid, the silicone oil has been known to exhibit viscoelastic behavior. Boger (Calabrese et al., 1986) determined that the silicone oil of 133 poise has a Weissenburg number of $We = 0.00088$ for $20 < G < 200\ s^{-1}$. Since the silicone oils used in this study have viscosities below 50 poise and the maximum operating shear rate of $G \sim 24\ s^{-1}$, any viscoelastic effect is expected to be negligible.

Initially, a drop of the dispersed phase is placed at the bottom of the cavity as shown in Figure 13, and mixing is induced by moving the top plate at various speeds. The initial drop size of $R = 0.363$ cm, and the volume fraction of $\phi_v = 0.008$ were used to prevent any significant coalescence effect.

The top plate is comprised of a synthetic fiber belt connected to a motor, which can attain the top speed of 16 cm/s. With a proper combination of the fluid system and the operating condition, the flow criterion of Reynolds number (Re) less than 1 can be achieved, in order to match the creeping flow condition of a real polymer system. The experimental

Table 1. Fluid Properties at 25°C

Sys. No.	Matrix Phase*	η_m (cp)	Dispersed Phase	η_d (cp)	η_d/η_m	σ (dyne/cm)
1	Silicone Oil 1000	975	Glycerin	210	0.215	25
2	Silicone Oil 5000	4,875		210	0.04	25
3	Silicone Oil 5000	4,875		750	0.154	25
4	Silicone Oil 500	487.5		750	1.54	25

*Dow Corning 200 fluids.

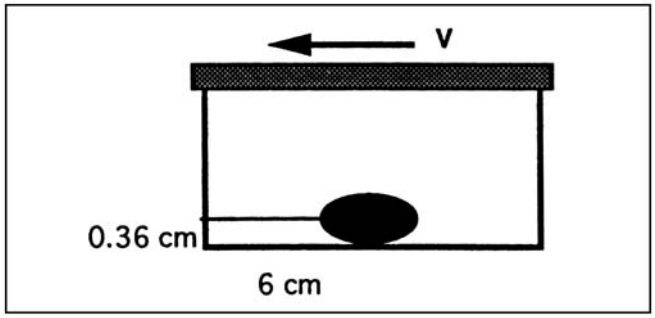

Figure 13. Initial position of the dispersed phase drop.

time is set at ~1 min or ~10 revolutions to achieve a steady-state condition. Since the initial drop position is in the zone B, the first couple of revolutions consists of elongation of the drop into a long thread in zone B. As the thread radius is reduced, breakup begins to occur, and the dispersed phase is gradually distributed into zone A. Therefore, the breakup in zone A does not occur until several revolutions have passed. Figure 14 delineates how the model cavity flow system is comparable to a real polymer processing system in the range of $1 \leq Ca \leq 10$.

One of the disadvantages of the experimental system is the inability to control the locations of the dispersed drops. Since the drops rarely travel the exact paths defined by the streamlines due to the flow disturbances provoked by the drop/drop interaction, the transfer of the dispersed phase occurs from zone B to A or vice versa. For instance, a drop originally located in zone A elongates into a thread may be caught between zone A and B, then as the thread relaxes and breaks up, the broken drops are separated distinctly into either of the zones based on their positions at the moment of the breakup. Because of the variations in drop positions during flow, it posed problems in the analysis.

The experimental results were obtained from taking still images and video recordings (Figure 15). Still images of the evolution of drop dispersion are taken with a 35 mm camera at the defined area in the low shear region as shown in Figure 16. Three 200 W bulbs are placed at the sides and the bottom of the cavity for a resolution of high quality. In this area, since most of the drops relax to form ellipsoidal shapes, these ellipsoidal shapes can be converted to the equivalent spherical shapes by the expression

$$R = \sqrt[3]{L \times B \times B} \tag{13}$$

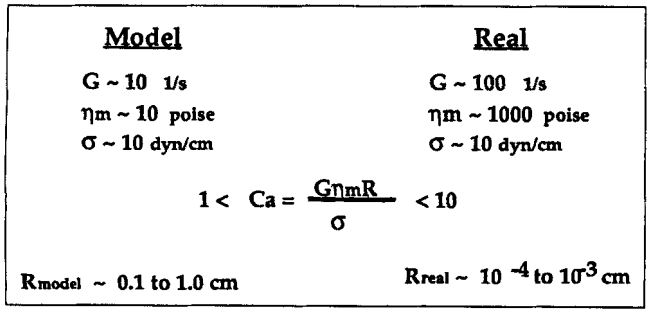

Figure 14. Operating conditions and the drop size: model vs. real systems.

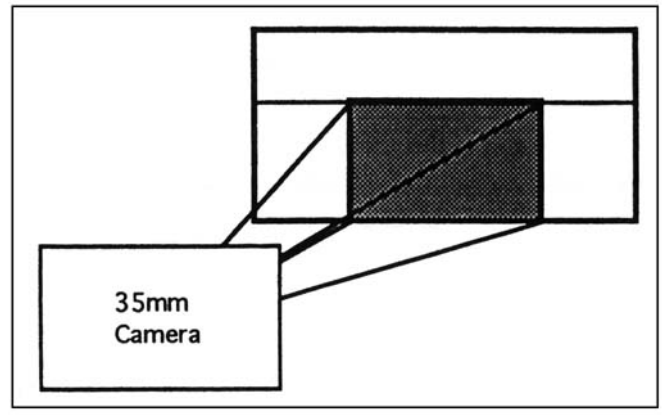

Figure 15. Images from the experiments.

Equation 13 assumes that the drops are symmetrical about the z-axis (Figure 4).

The video recordings on the experiments were captured to support the still images and also, the slow motion of the evolution of the drop breakup was used to fit the Tomotika's model.

The quantitative analysis of the images was carried out by scanning the still images and digitizing the images into a computer, where the images are processed using NIH Image 1.44 software. Using NIH Image 1.44, particle analysis was conducted to obtain particle area, dimension, position, angle of orientation, and so on. Then the obtained data were used as text format for further statistical analysis.

Results

In an earlier section, the different breakup mechanisms were discussed based on the different stream zones inside the cavity flow. In this section, we intend to support the breakup mechanism proposals with the experimental results of the particle analysis. In any particle-size analysis in polymer processing, it is always critical to understand the subtlety behind the size distribution and the evolution of the distribution. In this study, we attempted to approach this problem by correlating the size distribution to the breakup mechanism, and depicting the evolutions of drop dispersion using an average drop size.

Often, it is difficult to arrive at a measure of drop size which appropriately represents the morphological development of a dispersive mixing blend. In this analysis, we have considered the number average d_n and volume average d_v, drop sizes as possible measures to depict the evolution of drop-size distribution. Figures 17a and 17b give the compar-

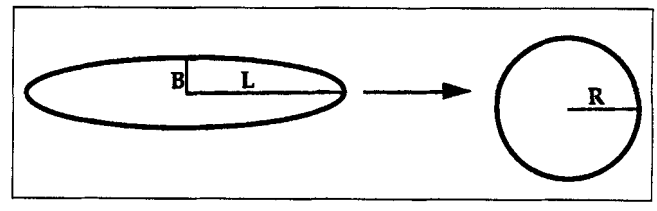

Figure 16. Ellipsoidal shapes from the image capturing area are converted into the spherical shapes.

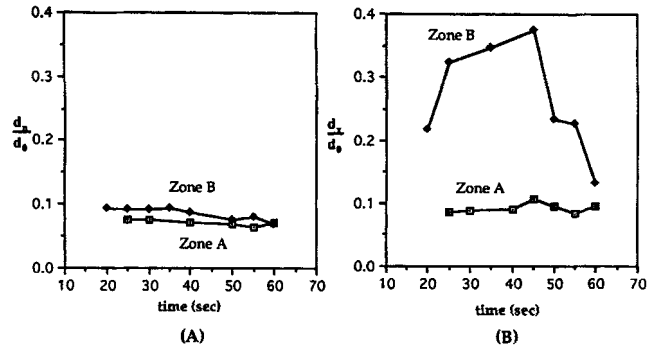

Figure 17. (A) Evolution of the number average drop sizes; (B) evolution of the volume average drop sizes in zone A and B at $V/H = 12\ s^{-1}$ and $\eta_r = 0.215$.

isons of the evolution of d_n and d_v in zone A and B. If one is not careful, Figure 17a may falsely lead to the conclusion that there is a little difference between zone A and B in their intrinsic natures of drop dispersion. Conversely, in Figure 17b, the comparison of d_v in zone A and B shows clearly the difference in the evolution due to the different shear histories experienced in zone A and B as discussed.

Therefore, d_v may be a suitable measure to represent the evolution since it depicts properly the evolution of the size distribution and distinguishes the evolution of zone A and B. In Figure 17b, the initial increase in drop size in zone B indicates the gradual formation of large drops from the extended thread. In the analysis, long threads, which have not yet formed into a measurable drop size, were neglected in the drop-size determination. After the drop size reaches the maximum, the drop size decreases continuously. In contrast, the drop size in zone A remains relatively steady. Although the drop size of zone B is always larger than the size of zone A, the disparity between the two stream zones diminishes to the minimum when flow ceases at $t \sim 60$ s. This occurs since some of the larger drops in zone B, unable to break up during the flow, disintegrate into smaller drops when the flow has stopped. This phenomenon indicates that since the most effective drop breakup occurs at flow cessation, the drop sizes become more evenly distributed in the cavity when flow is ceased than present.

Hence, the evolution of size distribution needs to be examined carefully since different stream zones display different size distributions related to their breakup mechanisms. As discussed earlier, the tip streaming mechanism is observed to be the dominant mechanism in zone B (Figure 18). The tip streaming produces a disparate drop-size distribution of numerous small drops and few large drops, where the sizes of the large drops are reduced slowly as shown in Figure 19. Again, it is important to note that flow cessation sufficiently reduces the drop sizes of the large drops in zone B and results in a narrower size distribution, comparable to zone A. In zone A, the size distribution is generally narrow and the size range remains consistent from the beginning to end of the process.

In Figure 10, the cavity was divided to three zones, where the attention was focused mainly on zone II. Because of the

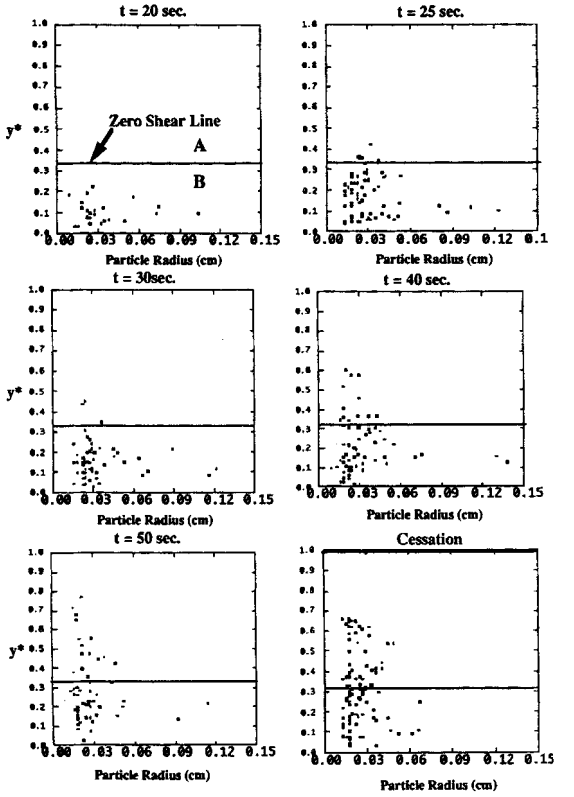

Figure 18. Evolution of drop-size distribution in zone A and B at $V/H = 12\ s^{-1}$ and $\eta_r = 0.215$.

The drop sizes are obtained from the experimental area indicated in Figure 15.

Fluid System 1

$\eta r = 0.215$
$\eta m = 9.75$ poise
$\sigma = 25$ dyn/cm
$ao = 0.01$ cm

Fluid System 2

$\eta r = 0.154$
$\eta m = 48.75$ poise
$\sigma = 25$ dyn/cm
$ao = 0.012$ cm

Fluid System 3

$\eta r = 0.04$
$\eta m = 48.75$ poise
$\sigma = 25$ dyn/cm
$ao = 0.008$ cm

Instability factor,

$q = 20.69$ $\quad$ $q = 4.04$ $\quad$ $q = 11.13$

	(1)		(2)		(3)	
ao (cm)	t (calc.)	t (obs.)	t (calc.)	t (obs.)	t (calc.)	t (obs.)
0.001	0.101 s		0.574 s		0.183 s	
0.0001	0.324 s	0.25 s	1.16 s	1.314 s	0.390 s	0.354 s

Assuming ao = 0.0001 cm

	(1)		(2)		(3)	
	Calc.	Obs.	Calc.	Obs.	Calc.	Obs.
λm (cm)	0.107	0.125	0.134	0.238	0.084	0.154
R (cm)	0.021	0.025	0.0185	0.0149	0.024	0.023

Figure 19. Sample calculations of the capillary breakup mechanism observed in zone II.

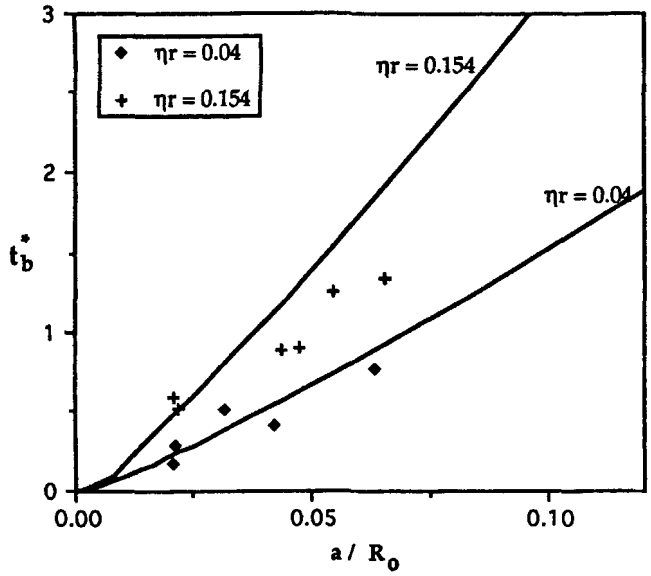

Figure 20. Predicted vs. observed values of the dimensionless breakup time for η_m = 4,875 cp.

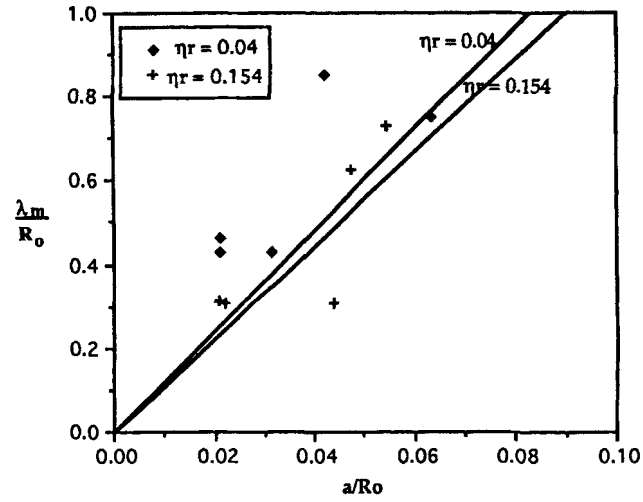

Figure 21. Predicted vs. observed values of the dominant wavelength λ_m.

shear history of high shear stress to near zero shear condition, zone II produces a breakup mechanism closely resembling the breakup mechanism indicated by Tomotika's breakup under flow cessation as the elongated threads broke up simultaneously with the end drops being little larger than the central drops. In Tomotika's model, an infinitely long cylindrical thread disintegrates into equally sized drops at regular intervals. However, Stone et al. (1986) reported that for a finitely long cylindrical thread, the end drops are somewhat larger than the central drops due to the "end-pinching" mechanism associated with internal pressure gradient induced by the capillary force. In Figure 18, the narrow size distribution in the vicinity of the zero shear line seems to indicate the breakup mechanism is primarily due to the capillary instability in zone II. To investigate further, the calculations for the drop breakup in zone II based on Tomotika's theory are shown in Figure 19. With an approximation on the value of α_0 (Janssen and Meijer, 1993; Rumscheidt and Mason, 1972), the measured values seem to agree well with the theoretical predictions.

Figure 20 shows the comparison of the calculated breakup times using Eq. 9 to the observed values for fluid systems 2 and 3 listed in Table 1. Because the capillary instability factor is inversely related to matrix phase, the breakup times for systems 1 and 4 could not be measured because the breakups occurred too fast due to the low matrix viscosities. The measurements were obtained in the low shear region near zone II. The observed values seem to support the theoretical values generally well. The figure shows that the observed breakup time values are smaller than the theoretical values.

In Figure 21, the dominant wavelength λ_m was measured and compared with the theoretical values. As shown in Figure 21, λ_m is a weak function of viscosity ratio and is not expected to change dramatically unless the viscosity ratio is varied by least an order of magnitude. Because of the constantly varying flow field, λ_m was very difficult to measure. However, the relatively close proximity between the measured and theoretical values seem to support the Tomotika phenomenon.

Figure 22 shows the comparison of the observed final drop sizes and the drop sizes predicted by the Tomotika theory. The observed drops were generally larger than the theoretical values. The deviation from the theory may be attributed to an inaccurate measurement of the thread radius a. Because of the constantly varying flow field, the threads rarely had uniform thread thickness, causing an inaccurate determination of the drop sizes. It needs to be emphasized that since the flow condition the cavity did not reproduce the Tomotika theory's flow condition of high shear followed by no shear, a deviation from the theoretical values was naturally expected.

In Figure 23, the evolution of d_v for zone I, II and III are given for the same experiment as in Figure 19. The evolution of zone III shows almost no difference from the evolution of zone B in Figure 13. However, the plots of zone I and II point out that a finer morphology is more likely to occur in

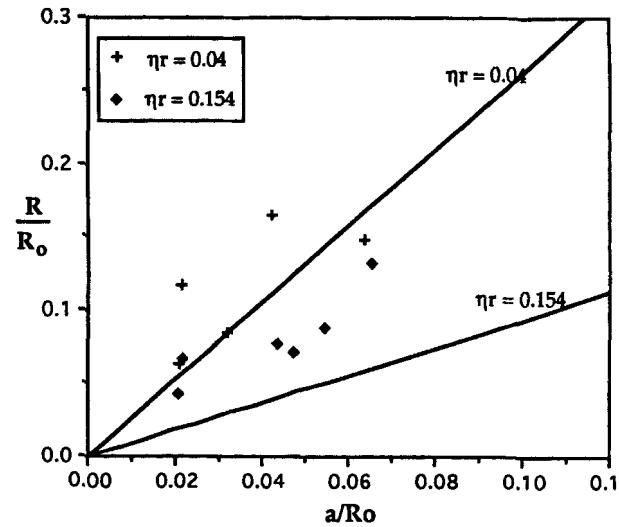

Figure 22. Predicted vs. observed values of the final drop sizes.

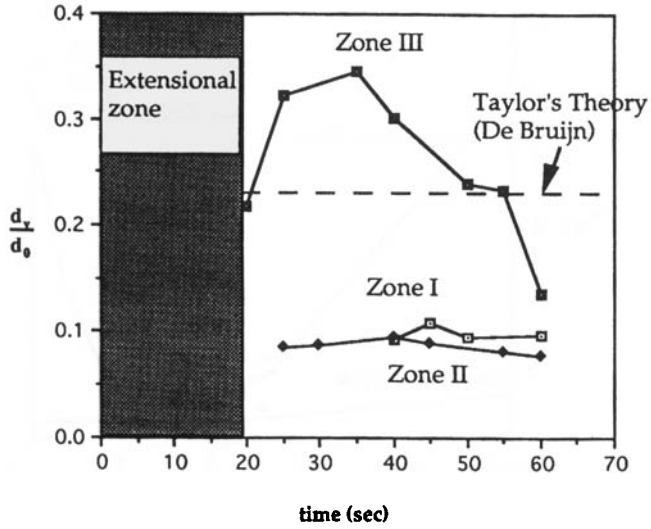

Figure 23. Evolution of volume average drop sizes in zones I, II and III at $V/H = 12\ s^{-1}$ and $\eta_r = 0.215$.

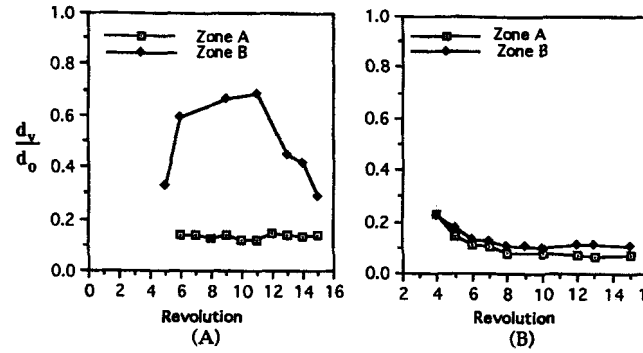

Figure 24. (A) Evolution of $\eta_r = 0.04$ at $V/H = 12\ s^{-1}$ ($\eta_d = 210$ cp and $\eta_m = 4{,}875$ cp); (B) evolution of $\eta_r = 0.215$ at $V/H = 12\ s^{-1}$ ($\eta_d = 210$ cp and $\eta_m = 975$ cp).

the vicinities of the zero shear line in zone II. The greater sizes in zone I than zone II also confirms Tomotika's theory, which indicates that a presence of flow (shear) hinders the capillary instability, and a sufficiently transient nature of shear is necessary for effective breakup. Figure 23 also shows that the drop sizes are much smaller than the prediction made by the Taylor theory, and this is indicative of how smaller drop sizes could be obtained by the transient breakup than by the steady breakup under a similar condition. Grace (1982) reported that in a static mixer, a sufficient drop-size reduction is achieved when shear is applied stagewise, with low shear holdup between stages to permit breakup of extended drops. The insertion of the relaxation zones improved the dispersion of $16 \sim 20$ folds and produced a much narrower drop-size distribution. Janssen and Meijer (1993) also showed that the capillary breakup mechanism is much more efficient and results in smaller drops than the Taylor's steady breakup mechanism under a similar condition.

Previous experimental studies on drop breakup explained the breakup phenomenon solely as a function of the viscosity ratio, and placed less emphasis on the actual viscosities of dispersed and matrix phases. In this study, it has been observed, in cavity flow, the matrix viscosity provides a significant influence on the breakup process. The effect of the matrix viscosity can be observed through Figures 24a and 24b. For the same dispersed viscosity and operating condition with different matrix viscosities, Figures 24a and 24b show how the evolution of zone A and B may be influenced by the rheological characteristic of the matrix phase and flow geometry. For $\eta_r = 0.04$ ($\eta_m = 4{,}875$ cp) in Figure 24b, the paths of the evolution of zone A and B are similar from the beginning to end of the dispersion process, and the difference in the drop sizes between zone A and B is not as significant as discussed in the earlier analysis. In contrast, for $\eta_r = 0.215$ ($\eta_m = 975$ cp) in Figure 24a, the evolution paths of zone A and B are quite different, and the disparity between the zones is greater than the former case. According to the steady breakup theory in a simple shear flow, a better breakup is supposed to occur for $\eta_r = 0.215$ than for $\eta_r = 0.04$ since the stress is more easily transferred across the interface for $\eta_r = 0.215$. However, by considering the transient breakup mechanism and the effect of the matrix viscosity in the cavity flow, the better breakup occurred for $\eta_r = 0.04$ than for $\eta_r = 0.215$ by improving the breakup phenomenon in zone B. For $\eta_r = 0.04$, the higher matrix viscosity imparted the drop with larger viscous force, which in turn led to a better elongation. And since the capillary instability is a weak function of the viscosity ratio but is inversely proportional to the matrix viscosity $q \sim 1/\eta_m$ (Eq. 4), the breakup time increased directly with the matrix viscosity $t_b \sim 1/q \sim \eta_m$ (Eq. 9). Therefore, the increase of the matrix viscosity resulted in a better elongation and better stabilization of the elongated threads. By stabilizing the elongated thread, the premature relaxation in the downward flight region was prevented, and a methodical relaxation was allowed to occur in the low shear region. Therefore, zone B's breakup process relies closely on the flow behavior in the downward flight region and is benefitted by the slower relaxation process provided by the higher matrix viscosity. This phenomenon indicates that the matrix viscosity is as an important parameter as the viscosity ratio in governing the breakup process.

According to the Tomotika theory, an increase in shear rate generally stabilizes the elongated thread and suppresses the relaxation process. In the cavity flow, increasing the shear rate may result in a better elongation but the transient effect may be reduced by raising the magnitude of shear rate in the low shear region. The effects of the shear rate for zone A and B are shown through Figures 25a, 25b, 26a, and 26b for viscosity ratios $\eta_r = 0.04$ and 1.54. Figures 25a and 26a show that a 50% increase of shear rate did not have much effect on the breakup process for $\eta_r = 0.04$. However, in Figures 25b and 26b, a greater effect of shear rate in zone A and B can be observed for $\eta_r = 1.54$. Also, for both viscosity ratios, zone B was affected more by the shear rate than zone A. Figures 25a, 25b, 26a and 26b show that the drop sizes are larger for $V/H = 18\ s^{-1}$ than for $V/H = 12\ s^{-1}$ during the flow. It seems that the shear rate imposed negative effects on the drop dispersion by stabilizing the elongated thread and suppressing the growth of capillary instabilities in the low shear region.

The issue of the relationship between final drop size and the change of apparent shear rate has been addressed in the

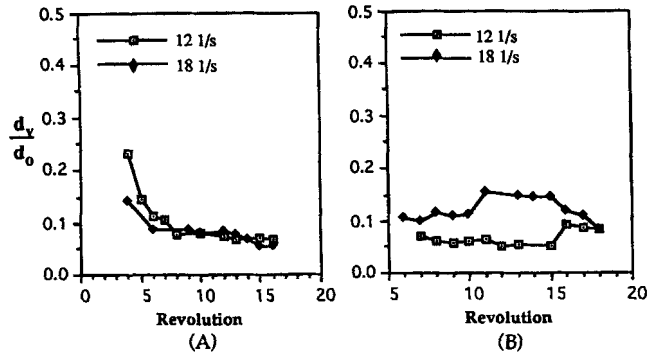

Figure 25. (A) Evolutions of $\eta_r = 0.04$ for zone A at $V/H = 12\ s^{-1}$ and $18\ s^{-1}$; (B) evolutions of $\eta_r = 1.54$ for zone A at $V/H = 12\ s^{-1}$ and $18\ s^{-1}$.

literature. Favis (1991) indicated that a factor of 2 or 3 has little or no effect on the morphology. Schreiber and Olguin (1983) showed that a tenfold increase of applied shear stress reduced the average drop size by a minimal amount. Yang (1994) also showed that, at higher volume fractions, the shear rate had a limited effect on mixing since the coalescence effect becomes dominant. On the other hand, Tomotika theory indicates, in order to produce a drop breakup via the transient breakup mechanism, it is only necessary to generate the thread radius sufficient enough to develop capillary instabilities in a low shear region. These findings indicate that the type of flow (transient or steady) may be more critical in the morphological development than the magnitude of applied shear stress. The problem these authors confront is that using a model based on a constant shear rate would require some other interpretation to explain the constant final particle size in spite of the change of apparent shear rate. The authors employed coalescence or elongational effects without considering these phenomena.

Finally, Figure 27 shows the comparison of Ca_{crit} values obtained from the final drop sizes in the cavity flow to the critical capillary curves of the simple shear and extensional flows. The figure shows that the experimental results fall within the limits of the two flows. It also shows that Ca_{crit} values of $18\ s^{-1}$ are generally greater than the values of $12\ s^{-1}$. This implies that the breakup efficiency in the cavity flow decreases as the shear rate increases. In Figure 27, the values

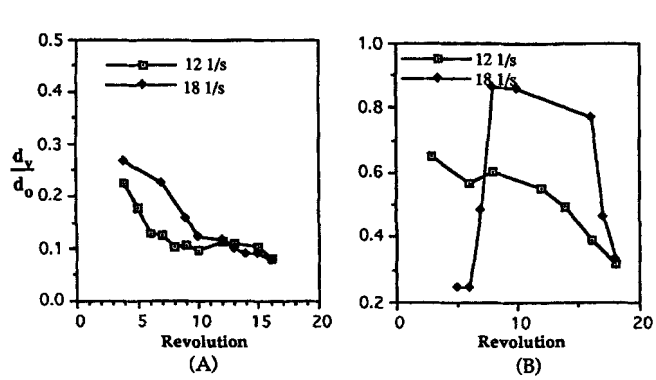

Figure 26. (A) Evolutions of $\eta_r = 0.04$ for zone B at $V/H = 12\ s^{-1}$ and $18\ s^{-1}$; (B) evolutions of $\eta_r = 1.54$ for zone B at $V/H = 12\ s^{-1}$ and $18\ s^{-1}$.

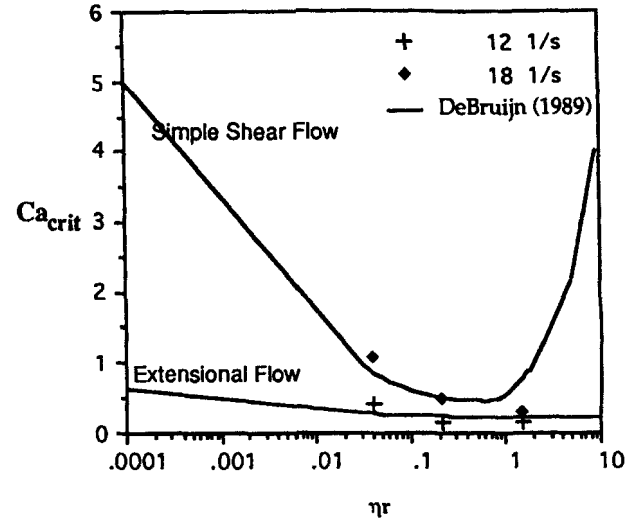

Figure 27. Critical capillary numbers from the experimental results: simple shear vs. extensional flow.

for $12\ s^{-1}$ fall near the extensional flow regime, while the values for $18\ s^{-1}$ are closer to the simple shear curve. These results again infer that the increase of shear rate does not necessarily improve the breakup phenomenon; instead, it may hinder the transient breakup process. Therefore, under an effective transient flow condition, the drop dispersion in the cavity flow may be as efficient or better than the extensional flow condition.

Conclusion

The nature of initial mixing of a two immiscible fluid system is studied in a 2-D rectangular cavity. The objective was to investigate drop breakup mechanisms induced by shear mixing in a fully transient flow field typical of a single-screw extruder. The nonuniform shear condition across the cavity channel produced drop sizes which varied with different stream zones. Because of the transient nature of flow in the cavity flow, Tomotika's theory based on the capillary instability seemed appropriate for describing the drop breakup phenomena in the cavity flow, especially near the streamline which passes through zero shear line at $y^* = 1/3$. The downward flight region imposed significant influences on the drop breakup due to the unfavorable flow conditions caused by a sudden shear reduction and an inversion of shear direction in zone B. Smaller d_v was detected in zone A than in zone B due to the favorable flow characteristics and limited flight effects. Therefore, in the outer streamlines (zone B), the breakup was harder to attain due to a long residence time in the downward flight region, and the tip streamlining breakup occurred instead of the methodical transient breakup. Hence, the drop breakup was found to be most optimal near the shear line because of the smooth transition from a high shear to no shear condition, and the breakup was least satisfactory at the outer streamlines. Since the transient breakup process was more dependent on the matrix viscosity than the viscosity ratio, a higher matrix viscosity resulted in a more evenly distributed dispersion phenomenon by delaying the breakup time

to inhibit the premature relaxation in the downward flight region. Finally, the increase of shear rate seemed to have a negative effect on the transient breakup process by suppressing the capillary instability during the flow. However, the final morphology seemed to be independent of the shear rate.

Acknowledgment

The authors acknowledge the members of the Polymer Mixing Program (GE Plastics, Welding Engineers, Inc., BF Goodrich, and Dow Chemical Co.). Without their support, this article would not have been accomplished. We also thank the student members in the program who provided invaluable moral and physical help to the results.

Notation

Ca_{crit} = Ca required for breakup to occur
d_o = initial drop diameter
d_n = number average drop diameter
d_v = volume average drop diameter
t_b = breakup time
t_b^* = dimensionless breakup time, $t_b^* = t_b G/Ca$
V/H = wall relative velocity
x = dimensionless wave number
$x^* = x/W$
$y^* = y/H$

Greek letters

α = disturbance amplitude
α_0 = initial disturbance amplitude
γ = strain imparted on drop
η_d = dispersed phase viscosity
η_r = viscosity ratio, η_d/η_m
λ_1 = relaxation time of dispersed phase for viscoelastic fluid
λ_2 = relaxation time of matrix phase for viscoelastic fluid
λ_m = wavelength associated with dominant instability
σ_o = interfacial tension of Newtonian fluid or flow absence

Literature Cited

Calabrese, R. V., T. P. K. Chang, and P. T. Dang, "Drop Breakup in Turbulent Stirred-Tank Contactors. Part I: Effect of Dispersed-Phase Viscosity," *AIChE J.*, **32**, 657 (1986).

Chella, R., and J. M. Ottino, "Fluid Mechanics of Mixing in a Single-Screw Extruder," *Ind. Eng. Chem., Fundam.*, **24**, 170 (1985).

Connor, J., "The Application of a Fundamental Mixing Theory," MS Thesis, Univ. of Maryland, College Park (1989).

Dann, J. R., "Forces Involved in the Adhesive Process: I. Critical Surface Tensions of Polymeric Solids as Determined with Polar Liquids," *J. Colloid Interf. Sci.*, **32**, 302 (1970).

De Bruijn, R., "Deformation and Breakup of Drops in Simple Shear Flows," PhD Diss., Eindhoven Univ. of Technology, Eindhoven, The Netherlands (1989).

Elemans, P. H. M., "Modelling of the Processing of Incompatible Polymer Blends," PhD Diss., Eindhoven Univ. of Technology, Eindhoven, The Netherlands (1989).

Favis, B. D., "Polymer Alloys and Blends: Recent Advances," *Can. J. Chem. Eng.*, **69**, 619 (1991).

Flumerfelt, R. W., "Drop Breakup in Simple Shear Fields of Viscoelastic Fluids," *Ind. Eng. Chem., Fundam.*, **11**, 312 (1972).

Grace, H., "Dispersion Phenomena in High Viscosity Immiscible Fluid Systems and Application of Static Mixers as Dispersion Devices," *Chem. Eng. Commun.*, **14**, 225 (1982).

Janssen, J. M. H., and H. E. H. Meijer, "Drop Breakup Mechanisms: Stepwise Equilibrium versus Transient Dispersion," *J. Rheol.*, **37**, 597 (1993).

Karam, H. A., and J. C. Bellinger, "Deformation and Breakup of Liquid Droplets in a Simple Shear Field," *Ind. Eng. Chem., Fundam.*, **7**, 576 (1968).

Mikami, T., R. G. Cox, and S. G. Mason, "Breakup of Extending Liquid Threads," *Int. J. Multiphase Flow*, **2**, 113 (1975).

Rowell, R. S., and D. Finlayson, "Screw Viscosity Pumps," *Engineering*, **114**, 606 (1922).

Rumscheidt, F. D., and S. G. Mason, "Particle Motions in Sheared Suspensions: XII. Deformation and Burst of Fluid Drops in Shear and Hyperbolic Flow," *J. Colloid Sci.*, **16**, 238 (1961).

Rumscheidt, F. D., and S. G. Mason, "Break-Up of Stationary Liquid Threads," *J. Colloid Interfac. Sci.*, **38**, 395 (1972).

Schreiber, H. P., and A. Olguin, "Aspects of Dispersion and Flow in Thermoplastic-Elastomer Blends," *Poly. Eng. Sci.*, **23**, 129 (1983).

Shi, Z. H., and L. A. Utracki, "Development of Polymer Blend Morphology During Compounding in a Twin-Screw Extruder," *Poly. Eng. Sci.*, **32**, 1834 (1992).

Stone, H. A., B. J. Bentley, and B. J. Leal, "An Experimental Study of Transient Effects in the Breakup of Viscous Drops," *J. Fluid Mech.*, **173**, 131 (1986).

Taylor, G. I., "The Formation of Emulsions in Definable Fields of Flow," *Proc. Roy. Soc.*, Ser. A 146, 501 (1934).

Tjahjadi, M., and J. M. Ottino, "Stretching and Breakup of Droplets in Chaotic Flows," *J. Fluid Mech.*, **232**, 191 (1991).

Tomotika, S., "Breaking up of a Drop of Viscous Liquid Immersed in Another Viscous Fluid which is Extending at a Uniform Rate," *Proc. Roy. Soc.*, Ser. A 153, 302 (1936).

Torza, S., R. G. Cox, and S. G. Mason, "Particle Motions in Sheared Suspensions: XXVII. Transient and Steady Deformation and Burst of Liquid Drops," *J. Colloid Interf. Sci.*, **38**, 395 (1972).

Ulrich, H., *Introduction to Industrial Polymers*, Hanser Publishers (1993).

Utracki, L. A., and Z. H. Shi, "Development of Polymer Blend Morphology During Compounding in a Twin-Screw Extruder: I. Drop Dispersion and Coalescence-Review," *Poly. Eng. Sci.*, **32**, 1824 (1992).

Yang, L., "Processing-Morphology Relationships in Blends of LLDPE and PS With and Without Compatibilizers," PhD Diss., Univ. of Maryland, College Park (1994).

Manuscript received Aug. 1, 1994, and revision received May 8, 1995.